

1 **Genetic homogeneity in the deep-sea grenadier *Macrourus berglax* across the North**
2 **Atlantic Ocean**

3 ***Authors***

4 Ilaria Coscia^{1,3*}, Rita Castilho², Alexia Massa-Gallucci³, Carlotta Sacchi³, Regina L.
5 Cunha², Sergio Stefanni⁴, Sarah J Helyar^{3,5}, Halvor Knutsen^{6,7}, Stefano Mariani^{1,3}

6

7 ¹ *School of Environment and Life Sciences, University of Salford, Salford,, Greater*
8 *Manchester, M5 4WT, UK*

9 ² *Center of Marine Sciences (CCMAR), University of Algarve, Faro, Portugal*

10 ³*School of Biology and Environmental Science, University College Dublin, Belfield, Dublin,*
11 *Ireland*

12 ⁴ *Stazione Zoologica A Dohrn, Villa comunale, Napoli, Italy*

13 ⁵ *Institute of Global Food Security, Queen's University Belfast, Belfast, Northern Ireland,*
14 *BT9 7BL, UK*

15 ⁶ *Centre of Coastal Research, University of Agder. Postboks 422, N-4604 Kristiansand,*
16 *Norway*

17 ⁷ *Institute of Marine Research, PO Box 1870, N5817 Bergen, Norway*

18

19 * Corresponding author: Ilaria Coscia (I.Coscia@salford.ac.uk), +44 (0)161 2957097

20 ***Keywords***

21 **Microsatellites, mitochondrial DNA, marine, population structure, fisheries**

22 ***Abstract***

23 Paucity of data on population structure and connectivity in deep sea species remains a major
24 obstacle to their sustainable management and conservation in the face of ever increasing
25 fisheries pressure and other forms of impacts on deep sea ecosystems. The roughhead
26 grenadier *Macrourus berglax* presents all the classical characteristics of a deep sea species,
27 such as slow growth and low fecundity, which make them particularly vulnerable to
28 anthropogenic impact, due to their low resilience to change. In this study, the population
29 structure of the roughhead grenadier is investigated throughout its geographic distribution
30 using two sets of molecular markers: a partial sequence of the Control Region of
31 mitochondrial DNA and species-specific microsatellites. No evidence of significant
32 structure was found throughout the North Atlantic, with both sets of molecular markers
33 yielding the same results of overall homogeneity. We posit two non-mutually exclusive
34 scenarios that can explain such outcome: i) substantial high gene flow among locations,
35 possibly maintained by larval stages, ii) very large effective size of post-glacially expanded
36 populations. The results can inform management strategies in this by-caught species, and
37 contribute to the broader issue of biological connectivity in the deep ocean.

38

39

40

41

42

43

44 ***Introduction***

45 Over the last few decades, it has become routine to use genetic techniques to
46 investigate population structure in marine fishes (Carvalho et al., 2016). The results have
47 led to the widespread rejection of the commonly held view that marine species are mostly
48 panmictic, due to the lack of visible barriers to larval and adult movements (Hauser and
49 Carvalho, 2008). The action of ocean circulation can in fact be two-fold: superficial or deep-
50 water currents can increase gene flow by aiding individual dispersal, especially at the larval
51 stages, but they can also act as a barrier to it, hence favouring divergence between groups.

52 The vast majority of published studies on marine fish have dealt with coastal pelagic
53 species, given their commercial value and/or the convenient sampling. Yet, the fishing
54 pressure on deep-sea stocks has been steadily increasing since the 1970s (Roberts, 2002),
55 and the depth at which fisheries operate has also been increasing at an average pace of 65.2
56 m per decade (Morato et al., 2006; Watson and Morato, 2013). Despite being increasingly
57 exploited, deep-sea fish species still suffer from a paucity of data, compared to their coastal
58 and shallow counterparts, which can have deleterious effects on their management (see
59 Clarke et al, 2015 for a quantitative discussion). The assessment of the level and range of
60 spatial structure of exploited species is pivotal for the sustainable harvest and management
61 of species, and failure to identify population structure may result in population collapse
62 (Reiss et al., 2009, Lowe and Allendorf, 2010). Given the typical life history traits of deep-
63 sea species (discrete spawning aggregations, slow growth, late maturity), any fishing
64 pressure might have serious consequences for the persistence of stocks (Baker et al., 2009).
65 Thus, it is important to gather data in order to better understand the population structure and
66 dynamics of these fish stocks, whether they are directly exploited or caught as by-catch. The
67 most recent studies on the dynamics of deep sea fish species have reported lack or very low
68 genetic structuring across wide geographical scales (*Centroscymnus crepidater* in Cunha et

69 al., 2012; *Coryphaenoides mediterraneus* in Catarino et al., 2013; *Hoplostethus atlanticus*
70 in White et al., 2009) across their vast geographic ranges, and capable of transoceanic
71 ontogenetic migrations (*Aphanopus carbo* in Longmore et al., 2014). Depth has been found
72 to represent a barrier to gene flow and promote low but significant population structuring
73 (*Haplostethus atlanticus* in Carlsson et al., 2011; *Etmopterus spinax* in Gubili et al., 2016;
74 *Coryphaenoides rupestris* and *Brosme brosme* in Knutsen et al., 2012, 2009; *Sebastes*
75 *mentella* in Shum et al., 2014, *Centroscymnus coelolepis* in Catarino et al., 2015). Although
76 the extent of pelagic habits typically influences the expected levels of genetic heterogeneity,
77 even at global scales (see Gaither et al, 2016), the deeper layers of the oceans remain less
78 understood, and no robust life-history predictors of spatial structure currently exist.

79 The roughhead grenadier *Macrourus berglax* Lacepède 1801, family Macrouridae, is
80 a benthopelagic species occurring across the northern Atlantic Ocean, between the Georges
81 Bank to the west, all the way to the Barents Sea as the easternmost edge. It dwells between
82 a depth of 100 and 1000 m, although it is especially common at depths of 300-500 m (Cohen,
83 1990). Data about its biology, population structure and dynamics are scarce, even though it
84 is an important part of the by-catch in the red fish and the Greenland halibut fisheries
85 (Garabana et al. 2016; Gonzales Costas and Murua, 2005; Gonzales costas 2010). Life
86 history traits of this species are similar to those of other deep sea fishes: it lives long (up to
87 25 years according to Lorance et al. (2008) and Drazen et al. (2012)), grows slowly and has
88 low fecundity, between 14,000 and 80,000 eggs (Devine et al., 2012; Fossen et al., 2003;
89 Murua, 2003, Drazen et al. 2012). Spawning has been documented across the species'
90 geographic distribution in late Winter/early Spring (Magnússon and Magnússon, 1995;
91 Savvatimsky, 1989), although geographical differences in time of spawning might exist
92 (Lorance et al., 2008; Garabana et al. 2016). Very little is known about the dispersal ability
93 at different life stages of *M. berglax*: spawning migration has been hypothesised (Garabana

94 et al. 2016), but not demonstrated. The other four species of the genus *Macrourus* (*M.*
95 *carinatus*, *M. whitsoni*, *M. caml* and *M. holotrachys*), are all present exclusively in the
96 southern hemisphere and have well-documented extended adult migration (Laptikhovsky
97 2011, Munster et al. 2016), while more distantly related macrourids, such as the roundnose
98 grenadier *Coryphaenoides rupestris*, have been found to have a very long pelagic phase,
99 which can last for almost a year (Lorance et al., 2008).

100 The population structure of *M. berglax* across its geographic range is also poorly
101 investigated. The only published genetic study finds low differentiation, but advocates the
102 existence of at least three units or stocks: East Greenland, West Greenland and Norwegian
103 Sea (Katsarou and Naevdal 2001). This investigation used allozyme markers, which, due to
104 their nature of being expressed by coding regions may poorly reflect patterns of neutral gene
105 flow (O'Sullivan *et al.*, 2003).

106 Concerns regarding the lack of data and the status of the stock of the roughhead
107 grenadiers in the North Atlantic were recently raised by NAFO (Northwest Atlantic
108 Fisheries Organization) and ICES (International Council for the Exploration of the Sea),
109 given the decrease in landings of grenadiers in the North Atlantic (Gonzales Costas 2010,
110 ICES 2015). In the NAFO Regulated Area (western Atlantic), this species is mainly caught
111 in subareas 3LMN, just around Flemish Cap, where it is becoming a commercially important
112 fish despite the fishery being unregulated (Gonzales Costas and Murua, 2005). In the eastern
113 Atlantic (ICES Area), it is by-caught with the roundnose grenadier *Coryphenoides rupestris*,
114 and its stock status is unknown and unmanaged (ICES 2015).

115 In this study, our aim was to fill some of these knowledge gaps by investigating the
116 population structure of the roughhead grenadier across its geographic range and over
117 multiple years, using species-specific microsatellite markers (Helyar et al., 2010) and the
118 mitochondrial DNA control region (CR). In particular, we tested whether spatial genetic

119 heterogeneity exists in *M. berglax*, and whether the three stocks suggested by Katsarou and
120 Naevdal (2001) are upheld by our data. The findings significantly enhance our
121 understanding of past and present population structure and diversification in *M. berglax*, and
122 lay the foundation for improved conservation and management of the species.

123

124 ***Materials and Methods***

125 *Sampling*

126 A total of 638 individuals were sampled at eight locations across the entire species'
127 geographic distribution, between 2000 and 2007 (Table 1), by research and commercial
128 vessels. The sampling localities are northern Norway (Bear Island), Svalbard, East and
129 South Greenland, Baffin Bay, Flemish Cap, Georges Bank and Hatton Bank (Fig. 1). Tissue
130 samples were collected and stored in absolute ethanol. Fork length was measured for each
131 individual at all except one location (Georges Bank). Finally, for all populations excluding
132 Georges Bank, anal fin length data was collected, and for Flemish Cap and South Greenland
133 individuals were sexed.

134 *Genetic analysis*

135 DNA was extracted from muscle tissue using a standard salting-out protocol (Miller et al.,
136 1988). A 1100 bp long fragment of the mtDNA Control Region (CR) was PCR amplified
137 from 124 individuals (Table 1) using primers L-Pro1 (Ostellari et al., 1996) and 12Sar-H
138 (Palumbi et al., 1991). All PCRs were carried out in a final volume of 25 μ l, containing 1X
139 PCR buffer (*Buffer BD Advantage 2 PCR* with $MgCl_2$), 0.2 mM of each dNTP, 0.2 μ M of
140 each primer, 1 μ l of template DNA, and Taq DNA polymerase (1 unit, *Taq BD Advantage™*
141 *2 Polymerase Mix*; CLONTECH-Takara). The following PCR profile was used for the
142 amplification: one cycle of 1 min at 95 °C, 35 cycles of 30 s at 95 °C, 30 s at 52 °C, and 70

143 s at 68 °C, and finally, one cycle of 5 min at 68 °C. PCR products were purified with an
144 ethanol/sodium acetate precipitation, and directly sequenced using the corresponding PCR
145 primers in an automated DNA sequencer (ABI PRISM 3700) using the BigDye Deoxy
146 Terminator cycle-sequencing kit (Applied Biosystems) following manufacturer's
147 instructions. Seven microsatellites (Helyar et al., 2010) were amplified for 559 individuals,
148 starting at 95°C for 15 min, followed by 35 cycles of 45 sec at 94°C, 45 sec at a set annealing
149 temperature, 45 sec at 72°C, and a final extension step of 45 min at 72°C. Markers were
150 multiplexed in 10 µl final volume using the QIAGEN Multiplex Kit as follows: 1) Mbe06,
151 Mbe02, Mbe03, Mbe04 at an annealing temperature of 57 °C; 2) Mbe01, Mbe08, Mbe10 at
152 60 °C. Both reactions were then run on an ABI3130xl genetic analyser for screening. Peaks
153 were scored using Genemapper 4.0 (Applied Biosystems).

154 *Statistical analysis*

155 Haplotype (h) and nucleotide (π) diversities and Φ_{ST} were calculated using Arlequin 3.5
156 (Excoffier and Lischer, 2010). Significance levels of all multiple statistical tests were
157 corrected using the false discovery rate (FDR) approach (Benjamini and Hochberg, 1995)
158 implemented in the QVALUE package (Dabney et al., 2010) in R (R Core Team, 2016).
159 Mitochondrial allelic richness (A_R) was estimated using the rarefaction method (El
160 Mousadik and Petit, 1996) as implemented in Contrib 1.02 (Petit and Pons, 1998). A median-
161 joining network (Bandelt et al., 1999) was calculated in PopART (<http://popart.otago.ac.nz>).
162 Mismatch analysis (Rogers and Harpending, 1992) was used to explore the demographic
163 history of the species, estimating both the raggedness index (rg, Harpending 1994) and the
164 sum of squared deviations (SSD, Schneider & Excoffier 1999) using Arlequin 3.5
165 (Excoffier and Lischer, 2010). Demographic mismatch analysis is based on the null
166 hypothesis of expansion; thus, non-significant values mean non-rejection of population

167 expansion. Initial and final θ estimates (before and after population growth or decline) and
168 τ values were calculated with ARLEQUIN 3.5 (Excoffier and Lischer, 2010). Time of
169 inferred population expansion was determined by $T_{\text{exp}} = \tau / (2 \mu n)$, where μ is the substitution
170 rate per base and per generation, and n the number of bases of the CR fragment (Rogers &
171 Harpending 1992), assuming a generation time of 15 years (Fossen et al., 2003). Historical
172 population size changes were further investigated by calculating Tajima's D and Fu's F_s
173 (Fu, 1997; Tajima, 1989a, 1989b) in ARLEQUIN 3.5.

174 The Bayesian Skyline Plot (BSP) approach as implemented in BEAST v 1.7 (Drummond
175 et al., 2012) was employed to estimate historical changes of female effective population
176 size. The best fitting model of substitution – HKY (Hasegawa et al., 1985) - was found
177 using jModelTest 0.1.1 (Guindon and Gascuel, 2003; Posada, 2008) via the Akaike
178 Information Criterion (AIC). Eight independent runs (each 10^6 generations and 10% burn-
179 in) were used to reach effective sample size value (ESS) of at least 200 as per the user's
180 manual.

181 For microsatellites, the frequency of null alleles was estimated using FreeNA (Chapuis and
182 Estoup, 2007). Marker neutrality was tested in LOSITAN (Antao et al., 2008) using the
183 approach described in Beaumont and Nichols (1996). GenAlEx v6 (Peakall and Smouse,
184 2006) was employed to estimate expected (H_E) and observed (H_O) heterozygosity indices.
185 Linkage disequilibrium, allelic richness (A_R), F_{IS} and F_{ST} were calculated in Fstat 2.9.3
186 (Goudet, 1995). Contemporary effective population size (N_e) was estimated using the
187 Linkage Disequilibrium method implemented in LDNe (Waples and Do, 2008), using 0.02
188 as minimum allowable allele frequency (P_{crit}). N_e was calculated both by location and
189 'overall', by pooling all the samples together based on the results. Population structure was
190 investigated using two approaches with different assumptions. STRUCTURE 2.3 (Falush et
191 al., 2007, 2003; Pritchard et al., 2000) was used to estimate population subdivision, allowing

192 for admixture and with both correlated and independent allele frequencies using 200,000
193 permutations following a burn-in of 50,000, with three independent runs for each value of
194 k . A second approach for estimating population structure, discriminant analysis of principal
195 components (DAPC), was implemented in the R package ADEGENET (Jombart, 2008;
196 Jombart et al., 2010). The optimal number of k clusters is chosen based on the associated
197 (lowest) Bayesian Information Criterion (BIC) calculated after 10^7 iterations. The difference
198 in these assignment tests lies in their assumptions: while STRUCTURE 2.3 groups
199 individuals in a number k of clusters by minimising Hardy-Weinberg (HWE) and linkage
200 disequilibria, DAPC groups individuals maximising the separation amongst such groups,
201 with no prior assumptions. COLONY (Jones and Wang, 2010) was used to estimate sibship
202 between sampled individuals, using Full Likelihood approach and remaining default
203 parameters. A threshold value of 0.8 was used, meaning that only pairs of individuals with
204 at least 80% probability of being fullsibs/halfsibs were considered (Bergner et al., 2014).
205 Although COLONY has proven to provide accurate results even with a low number of
206 markers (Harrison et al. 2013), given the low diversity of the present dataset the probability
207 of Type I errors cannot be disregarded (Taylor 2015). Thus, we performed the sibship
208 analysis with another package, ML-Relate (Kalinowski et al. 2006). Only the pairs identified
209 as sibs by both analyses were considered as such.

210

211 ***Results***

212 **Fork length.** Baffin Bay individuals were significantly smaller than individuals from all the
213 other populations (Fig. 5 and Fig. 3 Supplementary Material), while northern Norway
214 comprised the largest individuals. The length frequency distributions show that the only
215 population with a bi-modal trend is Svalbard.

216 **Mitochondrial Control Region.** A total of 29 haplotypes were identified in the 114
217 individuals sequenced across eight locations (GenBank accession Numbers: MG702365-
218 MG702488). All the diversity indices calculated for the mitochondrial DNA were found to
219 be lowest for Svalbard, with $h = 0.19$ and $\pi = 0.0002$. Haplotype diversity, nucleotide
220 diversity and the average number of nucleotide differences were highest for Flemish Cap,
221 being respectively 0.82, 0.0018 and 1.45. Allelic richness ranged from 1 (Svalbard) to 5.6
222 (Baffin Bay) (Table 1). The median-joining network showed haplotypes were grouped in a
223 clear star-like pattern. The most common haplotype was present in 86 individuals (75.4%
224 of the total) scattered across all sampled locations (see Fig. 1). Low but significant Φ_{ST}
225 were recorded between Svalbard and Flemish Cap (Table 2), but, given the low level of
226 genetic differentiation, demographic tests were performed for all samples pooled. Results
227 indicate that the Atlantic populations of *M. berglax* conform to both the demographic and
228 spatial expansion models ($P_{DEM} = 0.929$; $P_{SPA} = 0.796$) (Fig. 1 Supplementary Material).
229 The τ values ($\tau_{DEM} = 0.723 - 99\%CI: 0-3.639$; $\tau_{SPA} = 0.318 - 99\%CI: 0.1-4.7$) inferred were
230 used to estimate times since expansion (t) for both scenarios assuming a divergence rate of
231 11% per million years (Patarnello et al., 2007) and a generation time of 15 years (Fossen et
232 al., 2003) in the Mismatch Calculator (Schenekar and Weiss, 2011). The findings suggest
233 that the grenadier started expanding demographically 8,000 years ago (7,919, 99%CI:
234 0-39,858) and then spatially less than 4,000 years ago (3,483, 99%CI: 1,150-52,377).
235 Tajima's D (-2.32, $P \ll 0.00$) and Fu's F_S ($-\infty$, $P \ll 0.00$), both negative and highly
236 significant, further confirmed this scenario of expansion. Historical female effective
237 population size inferred with BEAST also indicated that expansion started ~4,400 years
238 ago (Fig 2).

239 **Microsatellites.** No evidence of null alleles and linkage disequilibrium was identified across
240 the microsatellite dataset. No significant departures from neutrality were detected in

241 LOSITAN when considering 99% confidence intervals. Expected heterozygosity H_E was
242 similar across locations, ranging between 0.619 (Hatton Bank) and 0.674 (Flemish Cap),
243 while the lowest H_O was recorded in Flemish Cap and Svalbard (0.53) and the highest in
244 Greenland (0.673 for South Greenland and 0.668 for Eastern Greenland). Heterozygote
245 deficiency ($H_O < H_E$) was detected in Svalbard and Flemish Cap, which indeed are the only
246 samples showing a positive and significant F_{IS} (Table 1). Pairwise F_{ST} values showed that
247 Norway was the most divergent population, with values that, despite being low, remained
248 significant after Bonferroni's correction. Other statistically significant pairwise comparisons
249 involved Svalbard against Baffin Bay and Georges Bank, and Georges Bank against South
250 Greenland (Table 2). Nevertheless, both assignment tests (STRUCTURE and ADEGENET)
251 employed failed to detect significant spatial population structure within the study area (Fig.
252 3 and Fig. 1 Supplementary Material). DAPC results did not show any significant
253 geographical pattern, even when repeated with populations grouped by year of capture (Fig.
254 3) or age class (data not shown). Effective population size was calculated both by location
255 and by pooling all the samples together, and every estimate had an infinite estimate of the
256 parameter. COLONY and ML-RELATE found 15 pairs of half-sibs and no full-sibs (Table
257 1 Supplementary Material and see Fig. 1 for a graphical representation) with no particular
258 pattern.

259 **Discussion**

260 The roughhead grenadier *Macrourus berglax* is an important part of the by-catch of halibut
261 and redfish fisheries, but is to some extent also targeted by smaller fisheries. Thus, in the
262 absence of a management plan, compounded with lack of information on the population
263 biology, any form of management strategy is hindered. The species is managed throughout
264 its range by two agencies, NAFO in the Northwest Atlantic and ICES in the Northeast
265 Atlantic. NAFO does not have specific regulations for the roughhead grenadier, and ICES

266 concludes that “no direct fishery should be allowed and that by-catch should be accounted
267 for against the TAC” (ICES, 2015).

268 In the only previously published work on population genetic structure of *M. berglax*,
269 Katsarou and Naevdal (2001) found low overall genetic diversity, but still called for each
270 subarea (West Greenland, East Greenland and Norway) to be managed as an independent
271 unit, as at least two out of the ten markers they used show heterogeneity. The authors called
272 for further investigations using more/different markers and a more intensive sampling
273 design. This has been implemented in the current study, where mitochondrial DNA and
274 nuclear hypervariable markers are simultaneously used, but still fail to support any evidence
275 of population structure. This aligns *M. berglax* with several other demersal and pelagic deep
276 sea fish species, such as the roundnose grenadier (White et al. 2010), the longnose velvet
277 dogfish (Cunha et al., 2012), the Mediterranean grenadier (Catarino et al., 2013) and the
278 black scabbard fish (Longmore et al. 2014), which were found to be largely genetically
279 homogeneous at oceanic level.

280 We used two different markers in order to investigate demographic processes at different
281 time scales: while the fast-evolving microsatellites are more suitable to untangle
282 contemporary structure (Hewitt, 2004), the mtDNA control region is usually employed to
283 unravel more ancient events on the evolutionary time scale, as well as track maternal
284 effects (being maternally inherited) (Awise, 2000). Hence, comparing and contrasting the
285 results from the two datasets can provide important insights into the processes that have
286 brought the species to be distributed as it is observed today.

287 From a management perspective, the lack of genetic differentiation at neutral markers
288 (microsatellites, markers not linked to parts of the genome under directional selection)
289 does not necessarily coincide with the existence of one single unit/stock. In marine
290 populations, low F_{ST} from neutral markers often reflect very large effective population size

291 in recently expanded populations, rather than the existence of substantial gene flow rates
292 (Cano et al., 2008), and this could be the case for the roughhead grenadier, whose
293 estimates of effective size are very large. In this scenario, even in the presence of low gene
294 flow, such large effective population size might be enough to counteract the divergence
295 caused by genetic drift, especially over a few generations, such as in the case of the slow-
296 growing *M. berglax*.

297 Comparing and contrasting the results from the two classes of markers used here, can
298 provide important insights into the processes that have shaped the genetic makeup of this
299 species. The mtDNA control region network shows a distinctive star-like shape, which is
300 an indication of demographic expansion. Two approaches with different assumptions have
301 been used to date such expansion, and both give the same time estimate: the roughhead
302 grenadier started expanding in the North Atlantic around 4,000 years ago. This
303 corresponds roughly to 200 generations, which in evolutionary scale is considered recent.
304 This timing is consistent with new habitat becoming available after the Younger Dryas
305 (~11,700 years ago). Unfortunately, based on the results, it is hard to speculate about the
306 possible location of the marine refugium which might have sourced the
307 recolonization/expansion into the North Atlantic Ocean (Kettle et al., 2011). It has been
308 hypothesised that the Atlantic Meridional Overturning Circulation (AMOC) went through
309 a strong spin-up after the last Younger Dryas glaciation and was responsible for one of the
310 most important dispersal events in the Atlantic, injecting larvae from the warmer southern
311 area, into ocean currents that led to the fastest postglacial range expansion ever recorded in
312 the deep (Henry et al., 2014).

313 The comparison between diversity indices calculated from both sets of molecular markers
314 (Table 1) allowed the determination of uneven contributions from the sampled populations
315 to the measured genetic diversity. Overall, microsatellite markers show consistent

316 homogeneity amongst locations. Mitochondrial DNA, on the other hand, shows that the
317 populations sampled at the western edge of the species distribution, Baffin Bay and Hatton
318 Bank, have the highest allelic richness and haplotypes diversity, contributing to the
319 majority of the total diversity. On the other hand, Svalbard registered the lowest values, for
320 any of the indices estimated from mtDNA (Table 2). Usually, lower genetic diversity,
321 hence lower adaptive capacity, is expected at population that originates from an expansion
322 (i.e. post-glacial) as they are subjected to a founder effect (Marko et al. 2010), compared to
323 those populations that still inhabits the refugial area (Diekmann and Serrao 2012). Yet,
324 supporting evidence is lacking (Zardi et al. 2015), so, once more, we cannot speculate on
325 the location of the refugium.

326 The F_{ST} analysis of microsatellites shows a low but statistically significant differentiation
327 of the Norwegian sample (Table 2). Having excluded the possibility of directional
328 selection acting upon these markers, we cannot conclude whether this is due to a spatial or
329 a temporal differentiation (these were the only fish caught in 2007). Nevertheless,
330 clustering analyses do not find Norway to be much different from the rest of the samples
331 (Fig. 2 Supplementary Material).

332 An interesting result unraveled by microsatellites is the presence of 15 half-sibs pairs
333 across the ocean. These are pairs of individuals born in different years that share at least
334 one parent. This could be explained by two possible causes: firstly, the roughhead
335 grenadier might have a unique spawning aggregation or secondly, and more likely, larval
336 and adult dispersal might play an important role in gene flow. Other members of the genus
337 *Macrourus* have been shown to have extended adult dispersal, and spawning migration has
338 also been hypothesized for *M. berglax* (Garabana et al. 2016). Adult dispersal and
339 migration have been shown to play an important role in ‘homogenizing’ populations, even

340 at oceanic scale (White et al. 2009), and could then explain the lack of genetic
341 differentiation detected in this study.

342 Lastly, the length distribution shows that the individuals caught in Baffin Bay are
343 significantly smaller than the ones coming from every other location (Fig. 4). This may
344 suggest that this area might be a breeding/nursery ground. Although this study can only
345 speculate about this, it would be important to consider this aspect in designing future
346 investigations, as this would be of vital importance for the management and conservation
347 of the species.

348 In conclusion, the roughhead grenadier *Macrourus berglax* shows no population structure
349 across the Atlantic Ocean. Whether this near-panmixia signal is due to a very large
350 population size or actual gene flow between locations is currently impossible to
351 disentangle. Nevertheless, caution should be taken when designing a management plan.

352 Previous studies using non-neutral markers did find significantly different units (Katsarou
353 and Naevdal, 2001), hence future work should aim at identifying markers under selection.

354 Local adaptation is now regarded as an important tool to discern populations in the marine
355 environment (Nielsen et al. 2012). Although this species is not a commercial target, it
356 makes up an important part of the bycatch, and more data should be gathered in order to
357 ensure its future conservation.

358

359 **Conflict of interest:** none

360

361 **Author contribution**

362 SM, RCa, HK and SS designed the study; IC analysed the data and wrote the manuscript
363 with input from SM and RCa; AMG, CS, SH and RCu conducted lab work; all authors
364 commented on drafts of the manuscript.

365

366 **Acknowledgements**

367 The authors would like to thank the members of all commercial and fishing expedition
368 through which samples for this study were collected.

369 This research has been funded as part of the DEECON project (EUROdeep, financially
370 supported by the European Science Foundation).

371 The author wish to thanks Francis Neat and Allan McDevitt for critical comments on the
372 manuscript draft, as well as the editor and two anonymous reviewers, whose work has
373 greatly improved the manuscript.

374

375

376 **References**

377 Antao, T., Lopes, A., Lopes, R.J., Beja-Pereira, A., Luikart, G., 2008. LOSITAN: a
378 workbench to detect molecular adaptation based on a FST-outlier method. *BMC*
379 *Bioinf* 9. doi:10.1186/1471-2105-9-323

380 Avise, J.C., 2000. *Phylogeography: the history and formation of species*. Harvard
381 university press.

382 Baker, K.D., Devine, J.A., Haedrich, R.L., 2009. Deep-sea fishes in Canada's Atlantic:
383 Population declines and predicted recovery times. *Environ. Biol. Fishes* 85, 79–88.
384 doi:10.1007/s10641-009-9465-8

385 Bandelt, H.J., Forster, P., Rohl, A., 1999. Median-joining networks for inferring
386 intraspecific phylogenies. *Mol. Biol. Evol.* 16, 37–48.

387 Beaumont, M.A., Nichols, R.A., 1996. Evaluating loci for use in the genetic analysis of

388 population structure. Proc. R. Soc. London B 263, 1619–1626.

389 Benjamini, Y., Hochberg, Y., 1995. Controlling the false discovery rate:/a practical and
390 powerful approach to multiple testing. J R Stat Soc B 57, 289–300.

391 Bergner, L.M., Jamieson, I.G., Robertson, B.C., 2014. Combining genetic data to identify
392 relatedness among founders in a genetically depauperate parrot, the Kakapo (*Strigops*
393 *habroptilus*). Conserv. Genet. 15, 1013–1020. doi:10.1007/s10592-014-0595-y

394 Cano, J.M., Shikano, T., Kuparinen, A., Merila, J., 2008. Genetic differentiation, effective
395 population size and gene flow in marine fishes: implications for stock management. J.
396 Integr. F. Sci. 5, 1–10.

397 Carlsson, J., Shephard, S., Coughlan, J., N. Trueman, C., Rogan, E., Cross, T.F., 2011.
398 Fine-scale population structure in a deep-sea teleost (orange roughy, *Hoplostethus*
399 *atlanticus*). Deep-Sea Res Pt I 58, 627–636. doi:10.1016/j.dsr.2011.03.009.

400 Carvalho, G.R., Hauser, L., Martinshon, J., Naish, K., 2016. Fish, genes and genomes:
401 contributions to ecology, evolution and management. J. Fish Bio. 89: 2471-2478.

402 Catarino, D., Stefanni, S., Menezes, G., 2013. Genetic diversity and length distribution of
403 the Offshore Rockfish (*Pontinus kuhlii*) from three Atlantic archipelagos and
404 seamounts. Deep-Sea Res Pt II 98: 160-169

405 Catarino, D., Knutsen, H., Veríssimo, A., Olsen, E.M., Jorde, P.E., Menezes, G., Sannæs,
406 H., Company, J.B., Neat, F., Danovaro, R., Dell’Anno, A., Rochowski, B., Stefanni,
407 S. 2015. The Pillars of Hercules as a bathymetric barrier to gene-flow promoting
408 isolation in a global deep-sea shark (*Centroscyrmnus coelolepis*). Mol Ecol 24: 6061-
409 79

410 Chapuis, M.P., Estoup, A., 2007. Microsatellite null alleles and estimation of population
411 differentiation. *Mol. Biol. Evol.* 24, 621–631.

412 Clarke, J., Millingan, R., Bailey, D., Neat, F., 2015. A scientific basis for regulating deep-
413 sea fishing by depth. *Curr Biol* 25: 2425-2429.

414 Cohen, D.M., 1990. Gadiform fishes of the world (order Gadiformes) : an annotated and
415 illustrated catalogue of cods, hakes, grenadiers, and other gadiform fishes known to
416 date. Food and Agriculture Organization of the United Nations.

417 Cunha, R.L., Coscia, I., Madeira, C., Mariani, S., Stefanni, S., Castilho, R., 2011. Ancient
418 Divergence in the Trans-Oceanic Deep-Sea Shark *Centroscymnus crepidater*. *PLoS*
419 *One* 7, e49196. doi:doi:10.1371/journal.pone.0049196

420 Dabney, A., Storey, J.D., Warnes, G.R., 2010. qvalue: Q-value estimation for false
421 discovery rate control. R Package Version 1.24.20.

422 Devine, J. a., Watling, L., Cailliet, G., Drazen, J., Durán Muñoz, P., Orlov, a. M.,
423 Bezaury, J., 2012. Evaluation of potential sustainability of deep-sea fisheries for
424 grenadiers (Macrouridae). *J. Ichthyol.* 52, 709–721.
425 doi:10.1134/S0032945212100062

426 Diekmann, O. E., and E. A. Serrao. 2012. Range-edge genetic diversity: locally poor
427 extant southern patches maintain a regionally diverse hotspot in the seagrass *Zostera*
428 *marina*. *Molecular Ecology* 21: 1647–1657.

429 Drazen J.C. & Haedrich R.L. (2012). A continuum of life histories in deep-sea demersal
430 fishes. *Deep-Sea Research I* 61: 34–42.
431

432 Drummond, A.J., Suchard, M.A., Xie, D., Rambaut, A., 2012. Bayesian phylogenetics

433 with BEAUti and the BEAST 1.7. Mol. Biol. Evol. doi:10.1093/molbev/mss075

434 El Mousadik, A., Petit, R.J., 1996. High level of genetic differentiation for allelic richness
435 among populations of the argan tree [*Argania spinosa* (L) Skeels] endemic to
436 Morocco. Theor. Appl. Genet. 92, 832–839.

437 Excoffier, L., Lischer, H.E.L., 2010. Arlequin suite ver 3.5: A new series of programs to
438 perform population genetics analyses under Linux and Windows. Mol. Ecol. Resour.
439 10, 564–567.

440 Falush, D., Stephens, M., Pritchard, J.K., 2003. Inference of population structure using
441 multilocus genotype data: linked loci and correlated allele frequencies. Genetics 164,
442 1567–1587.

443 Falush, D., Stephens, M., Pritchard, J.K., 2007. Inference of population structure using
444 multilocus genotype data: dominant markers and null alleles. Mol. Ecol. Notes 7,
445 574–578.

446 Fossen, I., Jørgensen, O.A., Gundersen, A.C., 2003. Roughhead grenadier (*Macrourus*
447 *berglax*) in the waters off East Greenland: Distribution and biology. J. Northwest Atl.
448 Fish. Sci. 31, 285–298.

449 Fu, Y.X., 1997. Statistical tests of neutrality of mutations against population growth,
450 hitchhiking and background selection. Genetics 147, 915–925.

451 Gaither, M.R., Bowen, B.W., Rocha, L.A., Briggs, J.C., 2016. Fishes that rule the world:
452 circumtropical distributions revisited. Fish Fish. 17, 664-679.

453 Garabana, D., Sampedro, P., Dominguez-Petit, R., Gonzales-Iglesias, C., Villaverded, A.,
454 Alvarez, M., Gonzalez-Tarrio, C., Hermida, M., 2016. A review of NAFO 3LMN

455 roughhead grenadier (*Macrourus berglax* Lacepede 1801) reproductive biology
456 including the evaluation of maturity ogive estimates. NAFO SCR Doc. 16.

457 Gonzales Costas, F., Murua, H. 2005. Assessment of roughhead grenadier, *Macrourus*
458 *berglax*, in NAFO Subareas 2 and 3. NAFO SCR Doc. 05/54, Serial No. N5140.

459 Gonzales Costas, F., 2010. An assessment of NAFO roughhead grenadier Subarea 2 and 3
460 stock. NAFO SCR Doc. 10/32, Serial No. N5790.

461 Goudet, J., 1995. FSTAT (Version 1.2): A computer program to calculate F-statistics. J.
462 Hered. 86, 485–486.

463 Gubili, C., Macleod, K., Perry, W., Hanel, P., Batzakas, I., Farrell, E.D., Lynghammar, A.,
464 Mancusi, C., Mariani, S., Menezes, G.M., Neat, F., Scarcella, G., Griffiths, A.M.,
465 2016. Connectivity in the deep: Phylogeography of the velvet belly lanternshark,
466 Deep Sea Research Part I: Oceanographic Research Papers.
467 doi:10.1016/j.dsr.2016.07.002

468 Guindon, S., Gascuel, O., 2003. A simple, fast, and accurate algorithm to estimate large
469 phylogenies by maximum likelihood. Syst. Biol. 52, 696–704.

470 Harpending, H.C., 1994. Signature of ancient population growth in a low-resolution
471 mitochondrial DNA mismatch distribution. Human Biology 66: 561-600.

472 Harrison, H.B., Saenz-Agudelo, P., Planes, S., Jones, G.P., Berumen, M.L., 2013. Relative
473 accuracy of three common methods of parentage analysis in natural populations. Mol
474 Ecol 22: 1158-1170.

475 Hasegawa, M., Kishino, H., Yano, T., 1985. Dating the human-ape splitting by a molecular
476 clock of mitochondrial DNA. J. Mol. Evol. 22, 160–174.

477 Hauser, L., Carvalho, G.R., 2008. Paradigm shifts in marine fisheries genetics: ugly
478 hypotheses slain by beautiful facts. *Fish Fish.* 9, 333–362.

479 Helyar, S., Sacchi, C., Coughlan, J., Mariani, S., 2010. Novel microsatellite loci for a deep
480 sea fish (*Macrourus berglax*) and their amplification in other grenadiers (Gadiformes:
481 Macrouridae). *Conserv. Genet. Resour.* 2, 1–4.

482 Henry, L.-A., Frank, N., Hebbeln, D., Wienberg, C., Robinson, L., de Flierdt, T. van, Dahl,
483 M., Douarin, M., Morrison, C.L., Correa, M.L., Rogers, A.D., Ruckelshausen, M.,
484 Roberts, J.M., 2014. Global ocean conveyor lowers extinction risk in the deep sea.
485 *Deep Sea Res. Part I Oceanogr. Res. Pap.* 88, 8–16.

486 Hewitt, G.M., 2004. Genetic consequences of climatic oscillations in the Quaternary.
487 *Philos. Trans. R. Soc. London* 359: 183-195.

488 ICES Advice, 2015. Roughhead grenadier (*Macrourus berglax*) in the North East Atlantic.
489 Copenhagen.

490 Jombart, T., 2008. Adegnet: a R package for the multivariate analysis of genetic markers.
491 *Bioinformatics* 24, 1403–1405.

492 Jombart, T., Devillard, S., Balloux, F., 2010. Discriminant analysis of principal
493 component: a new method for the analysis of genetically structured populations.
494 *BMC Genet.* 11, 94.

495 Jones, O.R., Wang, J., 2010. COLONY: a program for parentage and sibship inference
496 from multilocus genotype data. *Mol. Ecol. Resour.* 10, 551–555.

497 Kalinowski ST, AP Wagner, ML Taper (2006). ML-Relate: a computer program for
498 maximum likelihood estimation of relatedness and relationship. *Mol. Ecol. Notes*

499 6:576-579.

500 Katsarou E and Naevdal G (2001). Population genetic studies of the roughhead grenadier,
501 *Macrourus berglax* L., in the North Atlantic Ocean. Fish. Res. 51, 207-215

502 Kettle, A.J., Morales-M Niz, A., Roselló-Izquierdo, E., Heinrich, D., Vøllestad, L.A.,
503 2011. Refugia of marine fish in the northeast Atlantic during the last glacial
504 maximum: concordant assessment from archaeozoology and palaeotemperature
505 reconstructions. Clim. Past 7, 181–201.

506 Knutsen, H., Jorde, P.E., Bergstad, O.A., Skogen, M., 2012. Population genetic structure
507 in a deepwater fish *Coryphaenoides rupestris*: Patterns and processes. Mar. Ecol.
508 Prog. Ser. 460, 233–246.

509 Knutsen, H., Jorde, P.E., Sannæs, H., Rus Hoelzel, A., Bergstad, O.A., Stefanni, S.,
510 Johansen, T., Stenseth, N.C., 2009. Bathymetric barriers promoting genetic structure
511 in the deepwater demersal fish tusk (*Brosme brosme*). Mol. Ecol. 18, 3151–3162.

512 Laptikhovsky, V. 2011. Migrations and structure of the species range in ridge-scaled rattail
513 *Macrourus carinatus* (Southwest Atlantic) and their application to fisheries
514 management. – ICES J. Mar. Sci., 68: 309–318.

515 Longmore, C., Trueman, C.N., Neat, F., Jorde, P.E., Knutsen, H., Stefanni, S., Catarino,
516 D., Milton, J.A., Mariani, S., Gillanders, B., 2014. Ocean-scale connectivity and life
517 cycle reconstruction in a deep-sea fish. Can. J. Fish. Aquat. Sci. 71, 1312–1323.

518 Lorance, P., Large, P. a, Bergstad, O.A., Gordon, J.D.M., 2008. Grenadiers of the
519 Northeast Atlantic - Distribution, biology, fisheries, and their impacts, and
520 developments in stock assessment and management. American Fisheries Society

521 Symposium 63, 365–397.

522 Lowe, W.H., Allendorf, F.W., 2010. What can genetics tell us about population
523 connectivity? *Mol. Ecol.* 19: 3038-3051.

524 Magnússon, J.V., Magnússon, J., 1995. The distribution, relative abundance, and biology
525 of the deep-sea fishes of the Icelandic slope and Reykjanes Ridge., in: Hopper, A.G.
526 (Ed.), *Deep-Water Fisheries of the North Atlantic Oceanic Slope*. Kluwer Academic
527 Publishers, Dordrecht, pp. 161–199.

528 Marko, P.B., J. M. Hoffman, S.A. Emme, T.M. McGovern, C.C. Keever, Cox, N.L., 2010.
529 The ‘Expansion–Contraction’ model of Pleistocene biogeography: rocky shores suffer
530 a sea change? *Mol. Ecol.* 19: 146–169.

531 Miller, S.A., Dykes, D.D., Polesky, H.F., 1988. A simple salting out procedure for
532 extracting DNA from human nucleated cells. *Nuc. Ac. Res.* 16.

533 Morato, T., Watson, R., Pitcher, T.J., Pauly, D., 2006. Fishing down the deep. *Fish Fish.* 7,
534 24–34.

535 Münster, J., Kochmann, J., Klimpel, S., Klapper, R., & Kuhn, T. (2016). Parasite fauna of
536 Antarctic *Macrourus whitsoni* (Gadiformes: Macrouridae) in comparison with closely
537 related macrourids. *Parasites & Vectors* 9: 403.

538

539 Murua, H., 2003. Population structure, growth and reproduction of roughhead grenadier on
540 the Flemish Cap and Flemish Pass. *J. Fish Biol.* 63, 356–373.

541 O’Sullivan, M., Verspoor, E., Wright, P.J., 2003. The potential for using molecular
542 techniques to determine population structure in marine finfish species of interest to
543 the Scottish industry. Fisheries Research Services Internal Report No 19/03.

544 Ostellari, L., Bargelloni, L., Penzo, E., Patarnello, P., Patarnello, T., 1996. Optimization of
545 single-strand conformation polymorphism and sequence analysis of the mitochondrial
546 control region in *Pagellus bogaraveo* (Sparidae, Teleostei): rationalized tools in fish
547 population biology. *Anim. Genet.* 27, 423–427

548 Palumbi, S., Romano, S., Mcmillan, W.O., Grabowski, G., 1991. The Simple Fool ' S
549 Guide To PCR. October 96822, 1–45.

550 Patarnello, T., Volckaert, F., Castilho, R., 2007. Pillars of Hercules: is the Atlantic-
551 Mediterranean transition a phylogeographical break? *Mol. Ecol.* 16, 4426–4444.

552 Peakall, R., Smouse, P.E., 2006. GENALEX 6: genetic analysis in Excel. Population
553 genetic software for teaching and research. *Mol. Ecol. Notes* 6, 288–295.

554 Petit, R.J., Pons, O., 1998. Bootstrap variance of diversity and differentiation estimators in
555 a subdivided population. *Heredity* 80, 56–61.

556 Posada, D., 2008. jModelTest: Phylogenetic Model Averaging. *Mol. Biol. Evol.* 25, 1253–
557 1256.

558 Pritchard, J.K., Stephens, M., Donnelly, P., 2000. Inference of population structure using
559 multilocus genotype data. *Genetics* 155, 945–959.

560 R Core Team, 2016. R: A Language and Environment for Statistical Computing.

561 Reiss, H., Hoarau, G., Dickey-Collas, M., Wolff, W.J., 2009. Genetic population structure
562 of marine fish: mismatch between biological and fisheries management units. *Fish
563 and Fish.*, 10, 361–395.

564 Roberts, C.M., 2002. Deep impact: The rising toll of fishing in the deep sea. *Trends Ecol.
565 Evol.* 17: 242-245.

566 Rogers, A.R., Harpending, H.C., 1992. Population growth makes waves in the distribution
567 of pairwise nucleotide differences. *Am. J. Phys. Anthropol.* 140, 552-569.

568 Savvatimsky, P.I., 1989. Investigations of roughhead grenadier (*Macrourus berglax* L) in
569 the northwest Atlantic, 1967–1983. *NAFO Sci. Coun. Stud.* 13, 45–51.

570 Schenekar, T., Weiss, S., 2011. High rate of calculation errors in mismatch distribution
571 analysis results in numerous false inferences of biological importance. *Heredity* 107,
572 511–512. doi: 10.1038/hdy.2011.48

573 Schneider, S., Excoffier, L. 1999. Estimation of past demographic parameters from the
574 distribution of pairwise differences when the mutation rates vary among sites:
575 application to human mitochondrial DNA. *Genetics* 152: 1079-1089.

576 Shum, P., Pampoulie, C., Sacchi, C., Mariani, S., 2014. Divergence by depth in an oceanic
577 fish. *PeerJ* doi:10.7717/peerj.525.

578 Taylor, Helen R., 2015. The use and abuse of genetic marker-based estimates of
579 relatedness and inbreeding. *Eco. and Evol.* 5.15: 3140–3150.

580 Tajima, F., 1989a. Statistical-method for testing the neutral mutation hypothesis by DNA
581 polymorphism. *Genetics* 123, 585–595.

582 Tajima, F., 1989b. The effect of change in population-size on DNA polymorphism.
583 *Genetics* 123, 597–601.

584 Waples, R.S., Do, C., 2008. LDNE: a program for estimating effective population size
585 from data on linkage disequilibrium. *Mol. Ecol. Resour.* 8, 753–756

586 Watson, R.A., Morato, T., 2013. Fishing down the deep: Accounting for within-species
587 changes in depth of fishing. *Fish. Res.* 140, 63–65.

588 White, T.A., Stefanni, S., Stamford, J., Hoelzel, A.R., 2009. Unexpected panmixia in a
589 long-lived, deep-sea fish with well-defined spawning habitat and relatively low
590 fecundity. *Mol. Ecol.* 18, 2563–2573.

591 Zardi, G.I., Nicastro, K.R., Serrão E.A., Jacinto, R., Monteiro, C.A., and Pearson, G.A.,
592 2015. Closer to the rear edge: ecology and genetic diversity down the core-edge
593 gradient of a marine macroalga. *Ecosphere* 6(2):23.

594

595

596

597

598

599

600

601

602

603

604

605

606

607

608

609

610 **Table 1** Sampling locations, population codes (*ID*), year of sampling (*Year*) and genetic
611 diversity parameters inferred from mitochondrial DNA and microsatellites. *N*, number of
612 individuals screened; *N_H*, number of haplotypes; *h*, haplotype diversity; π , nucleotide
613 diversity; *A_r*, allelic richness; *N_A*, number of alleles; *H_o*, observed heterozygosity; *H_E*,
614 expected heterozygosity; *F_{IS}*, inbreeding coefficient (in bold, values that are significant;
615 $p < 0.05$).

Location	ID	Year	Mitochondrial DNA					Microsatellites					
			N	N _H	h	π	<i>A_r</i>	N	N _A	<i>A_r</i>	<i>H_o</i>	<i>H_E</i>	<i>F_{IS}</i>
East Greenland	EGree	2000	12	5	0.58	0.0014	2.73	95	9.86	5.14	0.668	0.665	-0.005
South Greenland	SGree	2003	25	6	0.30	0.0006	1.92	88	9.57	4.88	0.673	0.650	-0.020
George Bank	GEO	2004	12	3	0.32	0.0004	1.67	52	7.86	4.96	0.599	0.649	0.070
Svalbard	SVA	2002	20	3	0.19	0.0002	1.00	80	8.26	5.02	0.535	0.668	0.200
Hatton Bank	HAT	2000	14	7	0.76	0.0015	4.51	50	7.71	4.82	0.592	0.619	0.040
Flemish Cap	FLE	2002	11	7	0.82	0.0018	3.08	21	5.43	4.89	0.530	0.674	0.210
Baffin Sea	BAF	2001	17	10	0.79	0.0017	5.56	75	9.14	4.77	0.637	0.646	0.010
Norway	NOR	2007	13	5	0.54	0.0009	3.07	98	7.29	4.64	0.623	0.629	0.010

616

617

618 **Table 2** Population pairwise comparisons: microsatellite-derived *F_{ST}* in the lower diagonal,
619 and mtDNA-based Φ_{ST} in the upper section. In bold, values that remain significant
620 ($p < 0.05$), and in bold and italic those that remain significant after Bonferroni's correction.

621

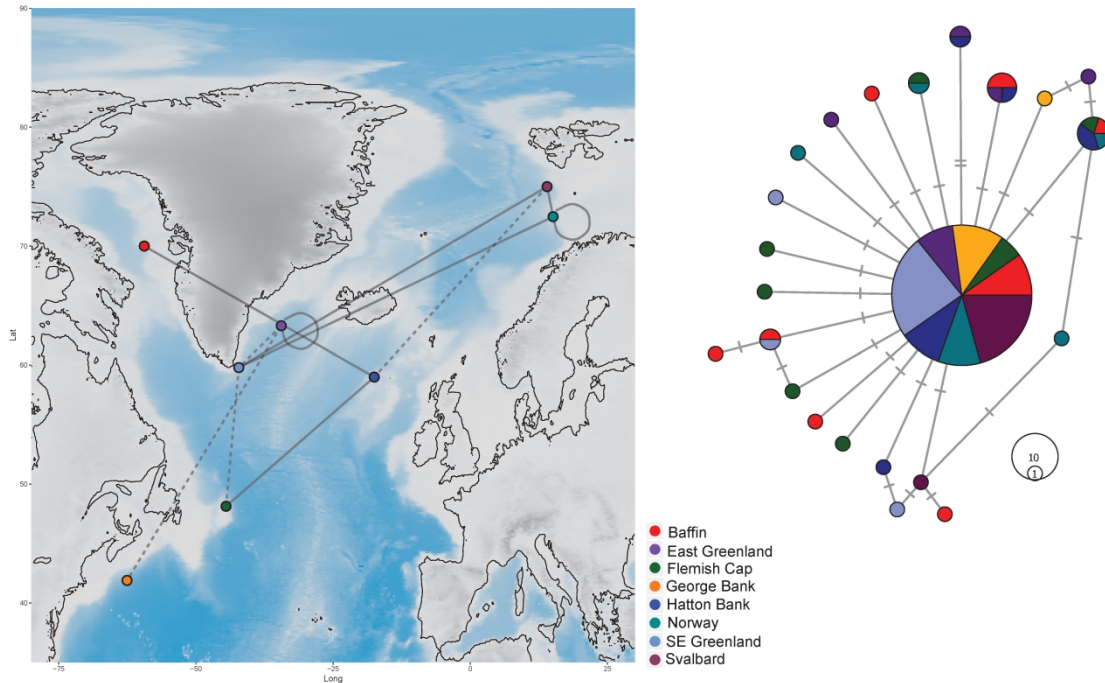
	$F_{ST} \setminus \Phi_{ST}$							
	Egree	Sgree	GEO	SVA	HAT	FLE	BAF	NOR
Egree	-	0.031	-0.02	0.035	-0.05	-0.01	-0.01	-0.01
Sgree	-0.0006	-	-0.012	-0.02	0.027	0.029	0.012	0.0307
GEO	-0.002	0.002	-	0.0091	0.009	0.057	0.0027	0.0228
SVA	0.003	0.005	0.001	-	0.0431	0.0448	0.0225	0.038
HAT	-0.007	0.001	0.0009	0.0096	-	-0.01	-0.01	-0.02
FLE	-0.002	-0.005	-0.001	-0.006	0.002	-	-0.006	-0.03
BAF	-0.003	-0.0008	-0.002	0.0045	-0.0007	-0.006	-	0.0225
NOR	0.0087	0.0068	0.0065	0.0049	0.0084	0.008	0.011	-

622

623

624

625

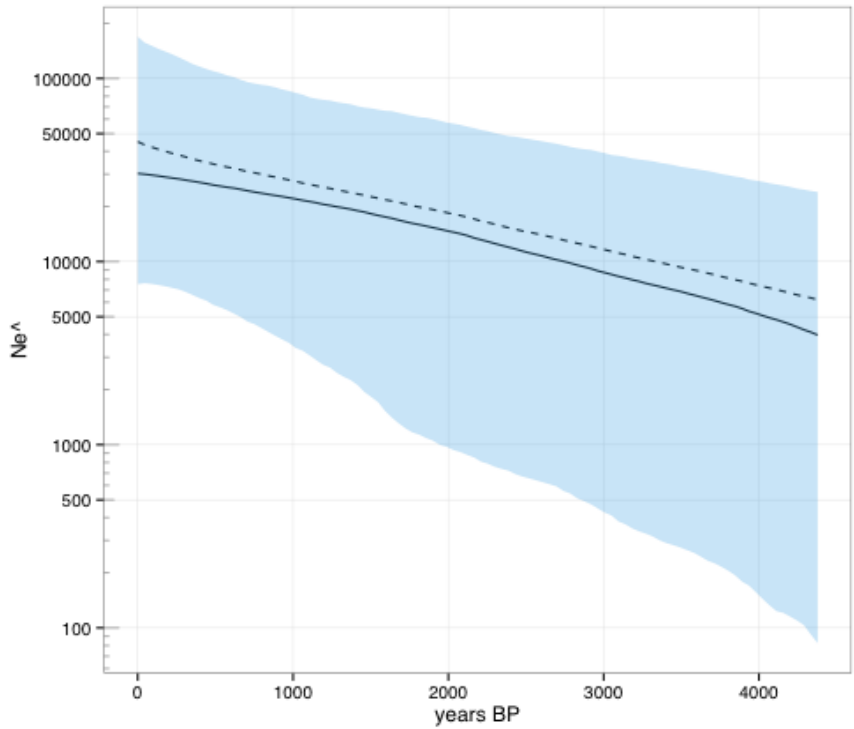


626

627 **Figure 1** Map showing the colour-coded sampling locations. The lines connecting the
628 locations represent the half-sib pairs: dashed lines for two pairs between locations, whereas
629 all the other lines represent one pair (see also Table 1 supplementary material). On the right,
630 the median-joining network of mitochondrial haplotypes.

631

632



633

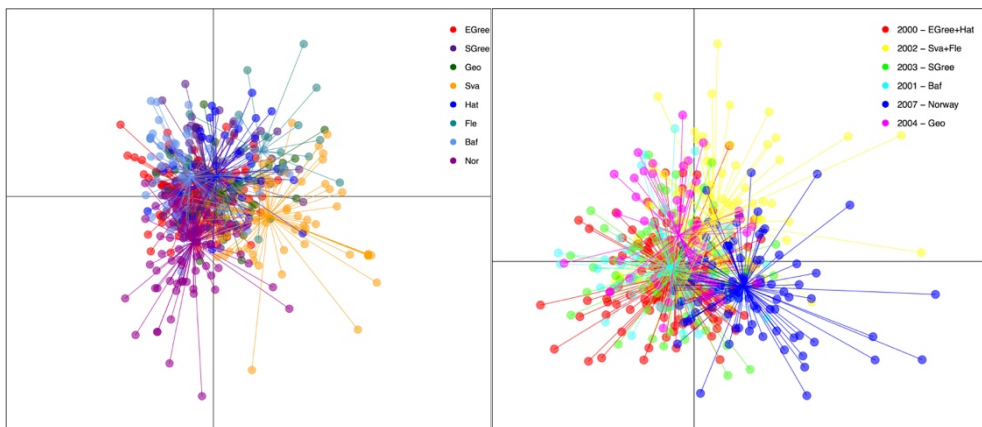
634 **Figure 2** Bayesian Skyline plot, showing the historical trend of female effective
 635 population size. The continuous and dashed lines represent the median and mean values,
 636 respectively. The shaded area represents the 95% Confidence interval.

637

638

639

640



641

642 **Figure 3** DAPC scatter plots by sampling locations (*left*) and year of capture (*right*). In the
 643 latter, the corresponding locations per year of capture are indicated in the legend.

644

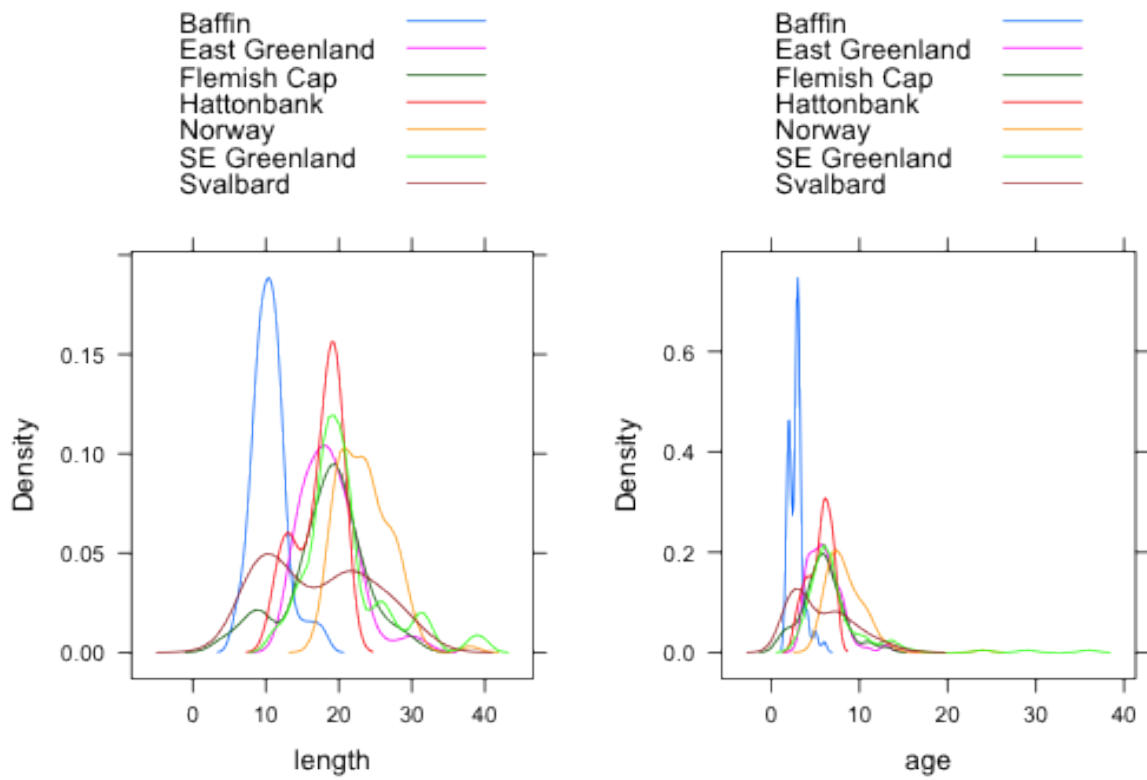
645

646

647

648

649



650

651 **Figure 4** Length frequency distributions by location.

652

653

654

655

656

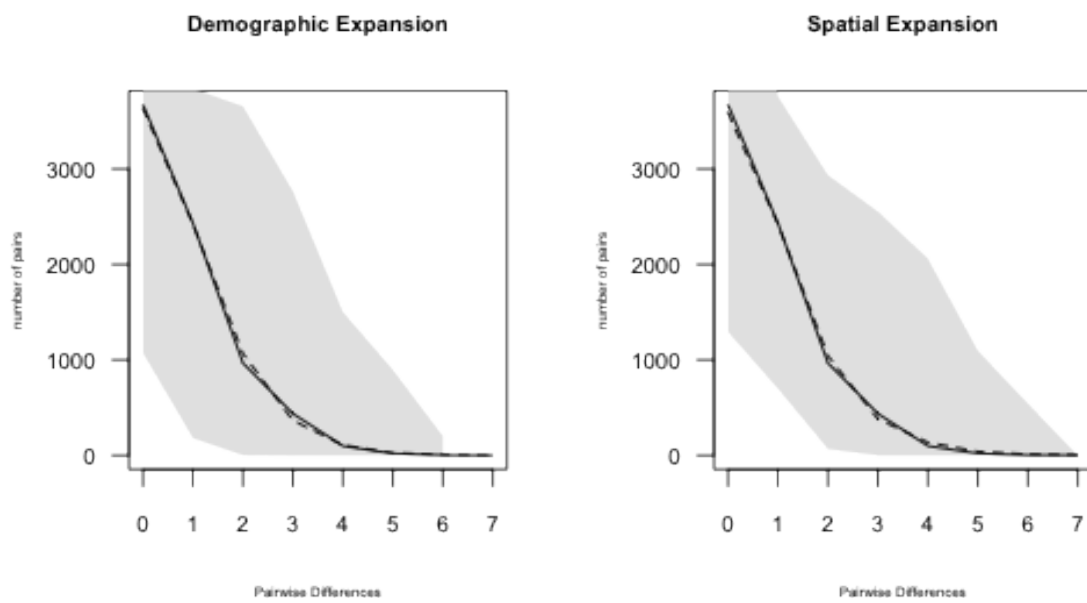
657

658

659

660

661 **Supplementary Material**



662

663 **Figure 1 Supplementary Material:** Mismatch distributions. The shaded grey area

664 represents the 95% confidence interval.

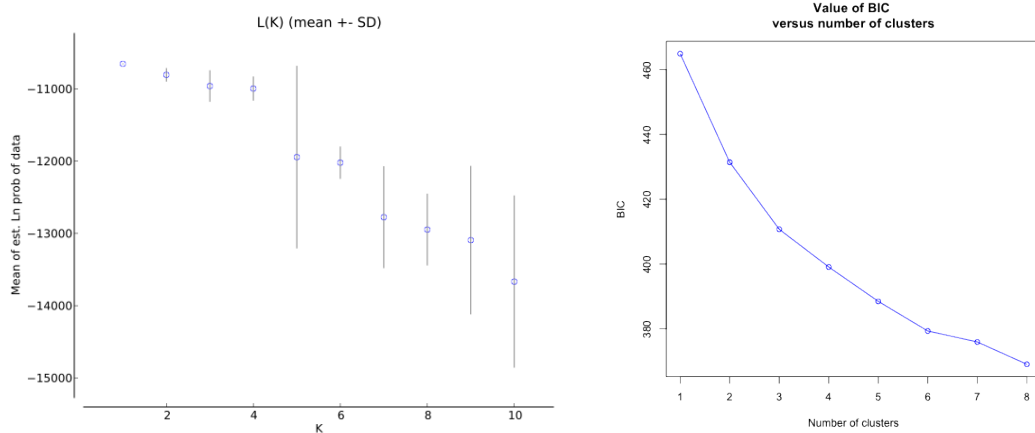
665

666

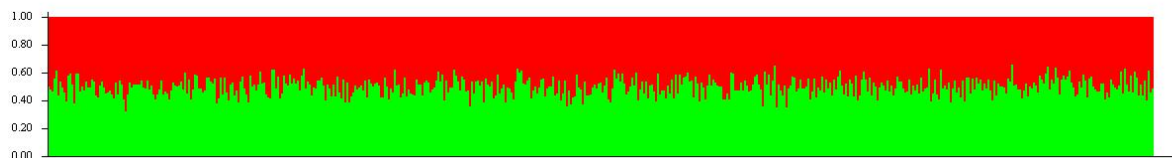
667

668

669



670



671

672 **Figure 2 Supplementary Material:** *Topleft* – Mean Likelihood inferred from
673 STRUCTURE; *topright* – graphical inference of the number of genetic clusters from DAPC.
674 Both graphs show a trend that is interpreted with the absence of genetic clusters
675 (homogeneity). This is particularly evident in the barplot at the bottom (inferred from
676 STRUCTURE): on the Y-axis the Q-value, and index of admixture; on the X-axis the
677 individuals.

678

679

680

681

682

683

684

685

686

687

688

689

690

691

692

693

694

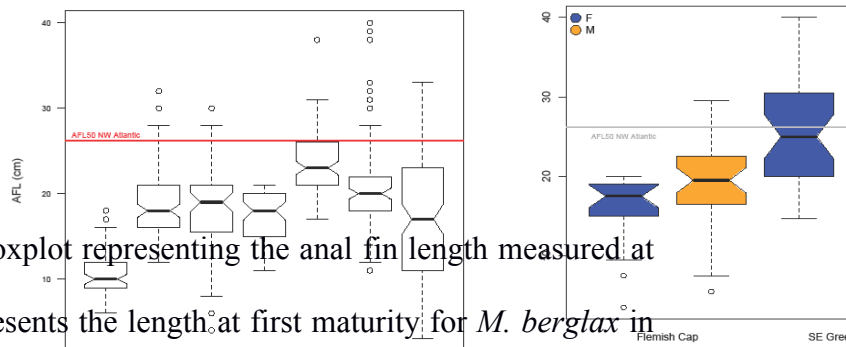


Figure 3 Supplementary Material: Boxplot representing the anal fin length measured at seven locations. *Left:* The red line represents the length at first maturity for *M. berglax* in the Atlantic. The notch in each box represents the 95% confidence interval. *Right:* length plotted by sex for two locations

695

696

697

698

699

Table 1 Supplementary Material. Half-sibs pairs detected and relative likelihood inferred from COLONY. Sibship analyses results: the combination of columns Off1 and Off2 indicate the pair of individuals for which a significant relationship has been found. The third column (Colony) contains the probabilities for such relationship. Colony has found only half-sibs in the datasets. The fourth column (ML-Relate) reports the findings of the ML-

700 Relate software. The latter confirms the half-sibs relationships. The only discrepancy is for
701 the pair Nor10-Nor48, which ML-Relate identify as Parent-Offspring pair.

Off1	Off2	Colony	ML-Relate
SGre5	Fle4	0.894	Half-Sib
Sva17	Hat28	0.884	Half-Sib
Hat27	Baf61	0.872	Half-Sib
EGre73	Geo49	0.868	Half-Sib
Sva10	Nor8	0.845	Half-Sib
EGre40	Geo46	0.840	Half-Sib
Sva25	Hat15	0.839	Half-Sib
SGre78	Sva57	0.832	Half-Sib
EGre26	EGre40	0.829	Half-Sib
SGre74	Nor6	0.823	Half-Sib
EGre53	SGre54	0.813	Half-Sib
Hat24	Fle9	0.810	Half-Sib
SGre39	Fle4	0.807	Half-Sib
Nor10	Nor48	0.807	Parent-Offspring
EGre63	SGre60	0.800	Half-Sib

702